

Phase Equilibrium Relationships in the System Gd_2O_3 – TiO_2

J. L. Waring and S. J. Schneider

(February 19, 1965)

The phase equilibrium relationships for a major portion of the Gd_2O_3 – TiO_2 system were determined in air, from a study of solid state reactions and from fusion characteristics. Three intermediate phases, a 1:2 compound, a 1:1 compound, and a face-centered cubic solid solution occur in the system. The solid solution phase is indicated on the phase diagram as existing from 33 to 40 mole percent TiO_2 , at 1750 °C. This phase melts incongruently over a range of temperatures and compositions, from 1840 °C, the peritectic temperature at 35 mole percent TiO_2 , to 1775 °C at 40 mole percent TiO_2 , the incongruent melting temperature of $Gd_2O_3 \cdot TiO_2$. The minimum temperature of stability for the phase is 1600 °C at 38 mole percent TiO_2 . The compound $Gd_2O_3 \cdot 2TiO_2$ has a cubic pyrochlore structure type with $a = 10.181 \text{ \AA}$ and melts congruently at 1820 °C. This phase apparently accepts up to about 3 mole percent TiO_2 in solid solution at 1460 °C. The compound $Gd_2O_3 \cdot TiO_2$, melts incongruently at 1775 °C and has a reversible phase transition at 1712 °C. The x-ray powder diffraction pattern of the high temperature modification was indexed on the basis of a hexagonal cell $a = 3.683 \text{ \AA}$, $c = 11.995 \text{ \AA}$ and is apparently related to the A-type rare earth oxide. The compositions $Sm_2O_3 \cdot TiO_2$ and $Eu_2O_3 \cdot TiO_2$ gave x-ray diffraction powder patterns with marked similarity one to the other as well as to both the high and low polymorphs of $Gd_2O_3 \cdot TiO_2$. The composition $Dy_2O_3 \cdot TiO_2$ formed several phases one of which is apparently related to the high temperature polymorph of $Gd_2O_3 \cdot TiO_2$.

1. Introduction

The increased availability of more pure rare earth oxides together with a continuing search for new rare earth refractory materials with desirable optical, electrical, and magnetic properties has served as an impetus to investigate the phase equilibrium relationships in rare earth oxide systems. The authors [1]¹ outlined, in part, the subsolidus relationships of the binary combinations of the rare earth sesquioxides with selected oxides of the trivalent cations.

It was decided to extend this rare earth sesquioxide study to incorporate the oxides of the tetravalent cations. For this reason, the system Gd_2O_3 – TiO_2 was selected to be studied in detail in air since it is probably representative of other B-type rare earth oxide– TiO_2 systems. The only detailed Ln_2O_3 – TiO_2 phase study² reported previously in the literature was that of the system La_2O_3 – TiO_2 by MacChesney and Sauer [2]. Roth [3] and Brixner [4] reported the existence of a number of rare earth titanates of the general type $Ln_2Ti_2O_7$ having the pyrochlore type structure, i.e., $Gd_2Ti_2O_7$ ($a = 10.181 \text{ \AA}$). Queyroux [5] reported a tentative phase diagram for the system Gd_2O_3 – TiO_2 in which three phases were postulated: a solid solution

phase occurring at approximately 40 mole percent TiO_2 , a 1:2 compound with limited solid solution, and a 1:1 compound.

Three polymorphs of Gd_2O_3 have been reported. They are the A (hexagonal), B (monoclinic) and C (cubic) type rare earth oxides. The A type was reported [6] to occur metastably. Several workers [7, 8] have reported that the C to B phase transition in Gd_2O_3 is reversible. Roth and Schneider [6] concluded that Gd_2O_3 crystallizes in the C form at low temperatures and transforms irreversibly to the B type at 1225 °C. In this study the B type was considered to be the only stable modification. The unit cell dimensions of B-type Gd_2O_3 were reported by Roth and Schneider [6] as $a = 14.06 \text{ \AA}$, $b = 3.572 \text{ \AA}$, $c = 8.75 \text{ \AA}$, and $\beta = 100.10^\circ$. Those of TiO_2 (rutile) were given by Swanson and Tatge [9] as $a = 4.594 \text{ \AA}$, $c = 2.958 \text{ \AA}$.

2. Materials

The starting materials used in this study were found by general quantitative spectrochemical analyses³ to have the following impurities: Gd_2O_3 –Ca present in amounts less than 0.01 percent, Fe, Mg, Pb, and Si each present in amounts less than 0.001 percent,

¹ Figures in brackets indicate the literature references at the end of the paper.

² The symbol "Ln" represents the lanthanide series, lanthanum through lutecium.

³ The spectrochemical analyses were performed by the Spectrochemical Section of the National Bureau of Standards. The rare earth oxides used to synthesize the related phases were better than 99.7 percent pure.

and B, Cu, and Mn each present in amounts less than 0.0001 percent. TiO_2 -Si present in amounts less than .1 percent, Mg present in amounts less than 0.01 percent, Cu present in less than 0.001 percent, and Ca present in amounts less than 0.0001 percent.

3. Specimen Preparation and Test Methods

Two gram batches of various combinations of Gd_2O_3 and TiO_2 were weighed, mixed in a mechanical shaker for approximately 10 min and pressed into disks at about 10^4 psi. The disks were placed on platinum setters and calcined in air at 1000°C for 18 hrs. To achieve physical homogeneity the specimens were ground in an agate mortar, repressed and recalced for an additional 4 hrs at 1000°C . Following these preliminary heat treatments portions of the ground specimen were placed in platinum alloy tubes and heated in the quenching furnace to various temperatures for different periods of time.

The tubes containing the specimens were quenched into ice water and examined by x-ray diffraction techniques. A high-angle recording Geiger counter diffractometer and Ni-filtered Cu radiation was used in the study. The Geiger counter traversed the specimen at $1/4$ deg/min and radiation was recorded on the chart at 1 deg- 2θ /in. The unit cell dimensions reported can be considered accurate to about ± 2 in the last decimal place listed. Equilibrium was considered to have been achieved when x-ray patterns showed no change after successive heat treatments of a specimen or when the data were consistent with the results from a previous set of experiments. Solidus and liquidus temperatures were obtained by using both a quenching furnace and an induction furnace. Because of the temperature limitation of the quenching furnace melting points above 1800°C were determined with the induction furnace. Some duplicate determinations below 1800°C were made using both furnace types.

The essential features of the furnaces were described previously by the authors [11]. In essence, the quenching furnace consisted of two concentric ceramic tubes wound with platinum-rhodium alloy wire. The inner tube served as the primary winding and the outer one as the booster. Separate power sources were used with each winding.

The power for the outer winding (booster) was supplied from a variable auto transformer. An a-c bridge type controller [12] in which the furnace winding was one arm of the bridge was used to control the temperature of the inner winding. The furnace temperature was controlled to about $\pm 3^\circ\text{C}$. Temperature was measured with a 95 percent Pt-5 percent Rh versus 80 percent Pt-20 percent Rh thermocouple used in conjunction with a high precision potentiometer.

The induction furnace consisted of an iridium crucible and cover which acted as the susceptor and specimen container. A small fragment of the calcined material was placed in the iridium crucible on an

iridium setter or button and heated to the desired temperature for about 2 min to achieve thermal equilibrium. Apparent temperatures were measured with a calibrated, disappearing filament-type optical pyrometer which was sighted through a 45 deg calibrated prism into the viewing hole at the center of the crucible cover. The temperature measuring system of both the quenching furnace and the induction furnace were calibrated frequently against the melting point of Au (1063°C), Pd (1552°C), and Pt (1769°C)⁴. In addition, the measuring system of the induction furnace was also calibrated against the melting point of Rh (1960°C). Temperatures reported in the present study were considered accurate to within $\pm 10^\circ\text{C}$ below 1650°C and to within $\pm 20^\circ\text{C}$ above. The measurements were reproducible to within $\pm 5^\circ\text{C}$, or better. The degree of melting was determined by the physical appearance of quenched or rapidly cooled specimens. The first adherence of the specimen to the platinum container or iridium setter generally established the beginning of melting. In quenched specimens, complete melting was established by the formation of a meniscus. Similarly the slumping or loss of shape of the inductively heated specimens established complete melting.

4. Results and Discussion

The equilibrium phase diagram (fig. 1) for a major portion of the Gd_2O_3 - TiO_2 system has been constructed from the data listed in tables 1 and 2. Solid circles represent composition and temperatures of experiments conducted in the quenching furnace and solid triangles represent those conducted in the induction furnace. A combination of a solid triangle bound by an open circle represents those conducted in both types of furnaces at the same temperature. Two melting points of Gd_2O_3 2330°C and 2350°C [13, 14] have been reported. Because of the temperature limitations of the present equipment the value was not redetermined. The numerous reported melting points of TiO_2 have been tabulated by Schneider [15]. Because of the apparent problems inherent with the determination of the melting point of TiO_2 , a redetermination was not made at this time.

The following intermediate phases, indicated in figure 1, were found to occur in the system: a solid solution (FCC_{ss}), existing at about 1750°C , from approximately 33 to 40 mole percent TiO_2 ; a compound, $\text{Gd}_2\text{O}_3 \cdot \text{TiO}_2$, and a compound $\text{Gd}_2\text{O}_3 \cdot 2\text{TiO}_2$. These data generally confirm those reported by Queyroux [5].

The solid solution phase (FCC_{ss}) has a maximum incongruent melting point at 1840°C at 35 mole percent TiO_2 . A minimum dissociation temperature was found to occur at 1600°C at 38 mole percent TiO_2 as compared to the 1550°C [5] value reported previously. The existence of a minimum decomposition temperature was evident since the solid solution phase once

⁴The purity of the metals used for calibration purposes was better than 99.9 percent. See reference [10].

formed could be decomposed by reheating to 1548 °C for 4 hrs. From x-ray powder diffraction data, the solid solution phase was shown to be face-centered cubic with a maximum unit cell dimension of 5.32 Å and a minimum of 5.28 Å at 1750 °C. Since the x-ray patterns were of rather poor quality with characteristic high background, the polarizing microscope was employed to determine the compositional limits of the phase. Small amounts of anisotropic phases were easily distinguished from the isotropic cubic phase.

The compound, $Gd_2O_3 \cdot TiO_2$, was found to melt incongruently at 1775 °C and to have a reversible phase transition at 1712 °C. The x-ray powder diffraction patterns for the low and the high temperature polymorphs of the 1:1 compound are given in tables 3 and

4 respectively. Unfortunately, neither of the x-ray patterns of the polymorphs of $Gd_2O_3 \cdot TiO_2$ could be indexed on a unit cell based on the constants given by Queyroux [5]. Without a more complete reporting of Queyroux's data these discrepancies cannot be resolved. The x-ray diffraction powder pattern of the low temperature form ($L-Gd_2O_3 \cdot TiO_2$) was not indexed. However, the x-ray diffraction pattern of the high temperature form ($H-Gd_2O_3 \cdot TiO_2$) was indexed on the basis of a hexagonal cell, $a=3.683 \text{ \AA}$, $c=11.995 \text{ \AA}$. The high temperature polymorph is apparently related to the hexagonal A-type rare earth oxide through the relationship c (hexagonal Ln_2O_3) $\cong \frac{1}{2} c$ ($H-Gd_2O_3 \cdot TiO_2$). Some difficulty was encountered in determining the inversion temperature since

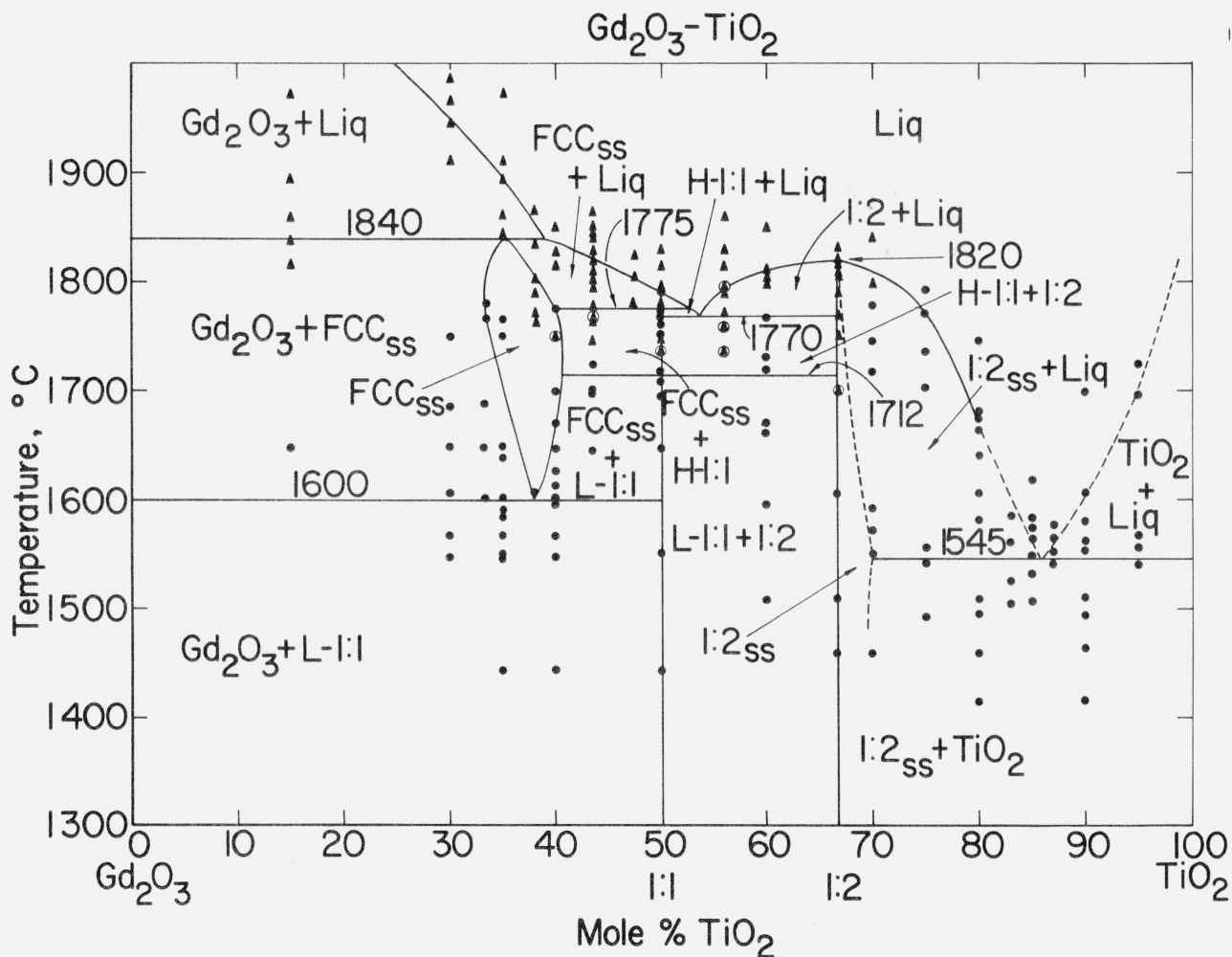


FIGURE 1. Phase equilibrium diagram for the system $Gd_2O_3-TiO_2$.

L-1:1—Low temperature form of $Gd_2O_3 \cdot TiO_2$.

H-1:1—High temperature form of $Gd_2O_3 \cdot TiO_2$.

1:2 — $Gd_2O_3 \cdot 2TiO_2$.

FCC — Face centered cubic phase.

ss — Solid solution.

Liq — Liquid.

● — Compositions and temperatures of experiments conducted in the quench furnace.

▲ — Compositions and temperatures of experiments conducted in the iridium crucible induction furnace.

● — Compositions and temperatures of experiments conducted in both the quenching and induction furnace.

For clarity, not all experimental data appearing in tables 1 and 2 are plotted on this diagram.

TABLE 1. Experimental quenching data for compositions in the Gd_2O_3 - TiO_2 system

Composition		Heat treatment ^a		X-ray analysis ^b	Remarks
Gd_2O_3	TiO_2	Temp.	Time		
Mole %	Mole %	°C	hr		
85	15	1648	2.5	$Gd_2O_3 + FCC_{ss}$	
70	30	1548	2	$L-Gd_2O_3 \cdot TiO_2 + Gd_2O_3$	
		1607	2.5	$FCC_{ss} + Gd_2O_3$	
		1648	2.5	$FCC_{ss} + Gd_2O_3$	
		1684	2.5	$FCC_{ss} + Gd_2O_3$	
		1751	2	$FCC_{ss} + Gd_2O_3$	
66.67	33.33	1601	2	$FCC_{ss} + Gd_2O_3^c$	
		1649	2	$FCC_{ss} + Gd_2O_3$	
		1688	3	$FCC_{ss} + Gd_2O_3$	
		1767	2	$FCC_{ss} + Gd_2O_3$	
		1781	4	FCC_{ss}	
65	35	1444	64	$L-Gd_2O_3 \cdot TiO_2 + Gd_2O_3$	
		1550	2	$L-Gd_2O_3 \cdot TiO_2 + Gd_2O_3$	
		1567	3	$L-Gd_2O_3 \cdot TiO_2 + Gd_2O_3$	
		1584	2	$L-Gd_2O_3 \cdot TiO_2 + Gd_2O_3$	
		1601	2.5	$FCC_{ss} + (Gd_2O_3)$	Gd_2O_3 not detected in x-ray pattern.
		1639	4	$FCC_{ss} + Gd_2O_3^c$	
		1648	3	$FCC_{ss} + Gd_2O_3$	
		1649	19	$FCC_{ss} + Gd_2O_3^c$	
		1751	1	FCC_{ss}	
		1767	2	FCC_{ss}	
		1548	5	$L-Gd_2O_3 \cdot TiO_2 + Gd_2O_3$	Reheat of 1648 °C specimen.
62	38	1606	6	FCC_{ss}	No microscopic evidence of second phase.
60	40	1444	64	$L-Gd_2O_3 \cdot TiO_2 + Gd_2O_3$	
		1567	3	$L-Gd_2O_3 \cdot TiO_2 + Gd_2O_3$	
		1599	16	$L-Gd_2O_3 \cdot TiO_2 + Gd_2O_3$	
		1601	2.5	$FCC_{ss} + (L-Gd_2O_3 \cdot TiO_2)$	$L-Gd_2O_3 \cdot TiO_2$ not detected by x-ray diffraction; presumed to be present on basis of other data.
		1613	1	$FCC_{ss} + L-Gd_2O_3 \cdot TiO_2$	
		1627	4	$FCC_{ss} + L-Gd_2O_3 \cdot TiO_2$	
		1648	3	$FCC_{ss} + (L-Gd_2O_3 \cdot TiO_2)$	$L-Gd_2O_3 \cdot TiO_2$ not detected by x-ray diffraction; presumed to be present on basis of other data.
		1672	2.5	$FCC_{ss} + L-Gd_2O_3 \cdot TiO_2^c$	
60	40	1700	1	FCC_{ss}	
		1751	2	FCC_{ss}	
		1776	66	FCC_{ss}	Specimen partially melted.
		1548	3	$L-Gd_2O_3 \cdot TiO_2 + Gd_2O_3$	Reheat of 1648 °C specimen.
56.45	43.55	1645	2.5	$FCC_{ss} + L-Gd_2O_3 \cdot TiO_2$	
		1698	6	$FCC_{ss} + L-Gd_2O_3 \cdot TiO_2$	
		1702	1	$FCC_{ss} + L-Gd_2O_3 \cdot TiO_2$	
		1724	3	$L-Gd_2O_3 \cdot TiO_2 + FCC_{ss} + H-Gd_2O_3 \cdot TiO_2$	Nonequilibrium mixture.
50	50	1444	64	$L-Gd_2O_3 \cdot TiO_2$	
		1550	2	$L-Gd_2O_3 \cdot TiO_2 + Gd_2O_3 + Gd_2O_3 \cdot 2TiO_2$	Nonequilibrium mixture.
		1648	2.5	$Gd_2O_3 \cdot 2TiO_2$	Do.
		1696	1.5	$Gd_2O_3 \cdot 2TiO_2$	Do.
		1708	1	$L-Gd_2O_3 \cdot TiO_2$	
		1708	2	$L-Gd_2O_3 \cdot TiO_2$	
		1718	2.5	$L-Gd_2O_3 \cdot TiO_2 + H-Gd_2O_3 \cdot TiO_2$	$H-Gd_2O_3 \cdot TiO_2$ present in small amount.
		1738	1	$L-Gd_2O_3 \cdot TiO_2 + H-Gd_2O_3 \cdot TiO_2$	Do.
		1751	1	$H-Gd_2O_3 \cdot TiO_2 + L-Gd_2O_3 \cdot TiO_2$	
		1760	1	$H-Gd_2O_3 \cdot TiO_2 + L-Gd_2O_3 \cdot TiO_2$	
		1777	.75	$H-Gd_2O_3 \cdot TiO_2 + L-Gd_2O_3 \cdot TiO_2$	Specimen partially melted $L-Gd_2O_3 \cdot TiO_2$ present in very small amount.
		1790	1	$H-Gd_2O_3 \cdot TiO_2 +$ unknown	Specimen partially melted. Extraneous x-ray peak $d = 3.0435 \text{ \AA}$ probably represents nonequilibrium phase.

TABLE 1. Experimental quenching data for compositions in the Gd_2O_3 - TiO_2 system—Continued.

Composition		Heat treatment ^a		X-ray analysis ^b	Remarks
Gd_2O_3	TiO_2	Temp.	Time		
Mole %	Mole %	°C	hr		
		1652	7	$L-Gd_2O_3 \cdot TiO_2$	Reheat of 1777 °C specimen. Reheat of 1790 °C specimen.
		1754	5	$H-Gd_2O_3 \cdot TiO_2 + L-Gd_2O_3 \cdot TiO_2$	
44	56	1737	3.5	$H-Gd_2O_3 \cdot TiO_2 + Gd_2O_3 \cdot 2TiO_2$	
		1762	.33	$H-Gd_2O_3 \cdot TiO_2 + Gd_2O_3 \cdot 2TiO_2$	
40	60	1508	3	$L-Gd_2O_3 \cdot TiO_2 + Gd_2O_3 \cdot 2TiO_2$	
		1597	2	$L-Gd_2O_3 \cdot TiO_2 + Gd_2O_3 \cdot 2TiO_2$	
		1662	5	$L-Gd_2O_3 \cdot TiO_2 + Gd_2O_3 \cdot 2TiO_2$	
		1670	4	$L-Gd_2O_3 \cdot TiO_2 + Gd_2O_3 \cdot 2TiO_2$	
		1720	3.5	$Gd_2O_3 \cdot 2TiO_2 + H-Gd_2O_3 \cdot TiO_2$	
		1730	1.5	$Gd_2O_3 \cdot 2TiO_2 + H-Gd_2O_3 \cdot TiO_2$	
33.33	66.67	1460	19	$Gd_2O_3 \cdot 2TiO_2$	
		1508	1	$Gd_2O_3 \cdot 2TiO_2$	
		1604	0.5	$Gd_2O_3 \cdot 2TiO_2$	
		1702	2	$Gd_2O_3 \cdot 2TiO_2$	
30	70	1460	19	$Gd_2O_3 \cdot 2TiO_{2ss} + TiO_2$	
20	80	1416	25	$Gd_2O_3 \cdot 2TiO_{2ss} + TiO_2$	
		1460	19	$Gd_2O_3 \cdot 2TiO_{2ss} + TiO_2$	
10	90	1416	25	$TiO_2 + Gd_2O_3 \cdot 2TiO_{2ss}$	

^a Unless otherwise indicated all specimens were first calcined at a 1000 °C–18 hr. and recalined at 1000 °C–4 hr.

^b Phases identified are given in order of amount present (greatest amount first) at room temperature.

^c Second phase identified by use of petrographic microscope.

TABLE 2. Melting characteristics of the Gd_2O_3 - TiO_2 system

Composition ^a		Temperature ^b	Furnace ^c	Observation
Gd_2O_3	TiO_2			
Mole %	Mole %	°C		
85	15	1816	I	Not melted.
		1839	I	Do.
		1860	I	Partially melted.
		1897	I	Do.
		1974	I	Do.
70	30	1911	I	Do.
		1946	I	Do.
		1967	I	Completely melted.
		1987	I	Do.
65	35	1838	I	Not melted.
		1841	I	Partially melted.
		1845	I	Do.
		1862	I	Do.
		1894	I	Completely melted.
		1911	I	Do.
1974	I	Do.		
62	38	1765	I	Not melted.
		1773	I	Do.
		1790	I	Do.
		1804	I	Partially melted.
		1835	I	Do.
		1867	I	Completely melted.
60	40	1751	Q	Not melted.
		1776	Q	Partially melted.
		1816	I	Do.
		1829	I	Do.
		1850	I	Completely melted.
56.45	43.55	1745	I	Not melted.
		1765	I	Do.
		1768	I	Do.
		1779	I	Partially melted.
		1796	I	Do.
		1803	I	Do.
1811	I	Do.		

TABLE 2. Melting characteristics of the Gd_2O_3 - TiO_2 system—Con.

Composition ^a		Temperature ^b	Furnace ^c	Observation
Gd_2O_3	TiO_2			
Mole %	Mole %	°C		
		1821	I	Completely melted.
		1830	I	Do.
		1841	I	Completely melted.
		1849	I	Do.
		1853	I	Do.
		1866	I	Do.
		1780	I	Partially melted.
		1805	I	Completely melted.
		1824	I	Do.
		1772	Q	Not melted.
50	50	1777	Q	Partially melted.
		1779	I	Do.
		1782	Q	Do.
		1795	I	Completely melted.
		1790	Q	Do.
		1814	I	Do.
1832	I	Do.		
44	56	1737	I	Not melted.
		1762	Q	Not melted.
		1762	I	Do.
		1773	I	Partially melted.
		1790	I	Do.
40	60	1796	I	Do.
		1797	Q	Do.
		1813	I	Completely melted.
		1830	I	Do.
		1862	I	Do.
		1996	I	Do.
		2050	I	Do.
		1767	Q	Not melted.
		1799	I	Partially melted.
		1806	I	Do.
1813	I	Completely melted.		
1849	I	Do.		

TABLE 2. Melting characteristics of the Gd₂O₃-TiO₂ system—Con.

Composition ^a		Temperature ^b °C	Furnace ^c	Observation
Gd ₂ O ₃	TiO ₂			
Mole %	Mole %			
33.33	66.67	1752	I	Not melted.
		1770	I	Do.
		1792	I	Do.
		1806	I	Do.
		1810	I	Do.
		1814	I	Do.
		1823	I	Melted.
		1834	I	Do.
		1843	I	Do.
		1850	I	Do.
		1878	I	Do.
30	70	1550	Q	Not melted.
		1573	Q	Partially melted.
		1592	Q	Do.
		1719	Q	Do.
		1747	Q	Do.
		1781	Q	Do.
		1798	I	Do.
		1840	I	Completely melted.
25	75	1490	Q	Not melted.
		1541	Q	Do.
		1555	Q	Partially melted.
		1704	I	Do.
		1736	I	Do.
		1772	I	Do.
		1794	I	Completely melted.
20	80	1495	Q	Not melted.
		1508	Q	Partially melted.
		1583	Q	Do.
		1606	Q	Do. ^d
		1641	Q	Do.
		1664	Q	Melted. ^d
		1677	Q	Do.
		1683	Q	Do.
		1747	Q	Do.
		1755	Q	Not melted.
17	83	1505	Q	Do.
		1525	Q	Melted. ^d
		1562	Q	Do.
		1585	Q	Do.
15	85	1506	Q	Not melted.
		1533	Q	Do.
		1549	Q	Melted. ^d
		1565	Q	Do.
		1575	Q	Do.
		1584	Q	Do.
		1618	Q	Do.
13	87	1542	Q	Not melted.
		1553	Q	Melted. ^d
		1564	Q	Do.
		1576	Q	Do.
10	90	1465	Q	Not melted.
		1495	Q	Do.
		1511	Q	Do.
		1554	Q	Partially melted.
		1561	Q	Do.
		1580	Q	Melted. ^d
		1608	Q	Do.
		1700	Q	Do.
5	95	1542	Q	Not melted.
		1556	Q	Partially melted.
		1568	Q	Do.
		1694	Q	Melted. ^d
		1725	Q	Completely melted.

^a Specimens first calcined at 1000 °C for 18 hr and recalined at 1000 °C for 4 hr.

^b Specimens furnace cooled except when indicated.

^c Q-quenching furnace; I-induction furnace. All specimens heated in induction furnace, slow cooled rather than quenched.

^d Definite verification of complete melting could not be obtained.

numerous attempts to quench H-Gd₂O₃·TiO₂ as a single phase below the solidus were unsuccessful. In each instance a small amount of L-Gd₂O₃·TiO₂ was present. However, the x-ray pattern of the partially melted 1:1 compound quenched from 1790 °C was found to be essentially single phase. One very weak extra line occurred in the x-ray pattern at $d = 3.044 \text{ \AA}$ which was probably representative of a

metastable phase formed only in the quenched liquid. Both the 33.33 and the 43.55 percent TiO₂ compositions when quenched from above 1712 °C, the inversion temperature of Gd₂O₃·TiO₂, contained H-Gd₂O₃·TiO₂ and an appropriate second phase. The same compositions quenched from below 1712 °C contained L-Gd₂O₃·TiO₂ and an appropriate second phase. These experimental data seem to indicate that the possibility of quenching H-Gd₂O₃·TiO₂ without residual traces of L-Gd₂O₃·TiO₂ is only accomplished by the presence of another second phase.

Other Ln₂O₃:TiO₂ compositions were also studied. From x-ray powder diffraction data, it appears that the compositions Sm₂O₃:TiO₂ and Eu₂O₃:TiO₂ form phases which are very similar to both L-Gd₂O₃·TiO₂ and H-Gd₂O₃·TiO₂. The composition Dy₂O₃:TiO₂ was found to contain a mixture of phases, one of which is apparently similar to H-Gd₂O₃·TiO₂. These related phases were not detected in the equimolar compositions of the oxides of the smaller rare earth cations with TiO₂.

The compound Gd₂O₃·TiO₂ was found to melt congruently at 1820 °C. From the change in unit cell constants with composition the compound apparently accepted up to about 3 mole percent TiO₂ in solid solution. The unit cell dimensions of the compositions Gd₂O₃:2TiO₂ and 30Gd₂O₃:70TiO₂ quenched from 1460 °C are 10.181 Å and 10.169 Å, respectively. Since the latter composition contained a small amount of TiO₂ the exsolution curve delineating the phase boundary is shown (fig. 1) as dashed at 69 percent TiO₂.

Earlier, the present authors [16] reported the parameters of the following Ln₂O₃·2TiO₂ pyrochlore-type phases: Eu₂O₃·2TiO₂ ($a = 10.195 \text{ \AA}$); Ho₂O₃·2TiO₂ ($a = 10.098 \text{ \AA}$); Er₂O₃·2TiO₂ ($a = 10.075 \text{ \AA}$); Tm₂O₃

TABLE 3. X-ray diffraction powder data for the low temperature modification of Gd₂O₃·TiO₂ (CuK_α radiation)

d^a	I/I_0^b
Å	
7.70	21
3.56	21
3.066	100
3.060	79
3.054	64
2.976	14
2.947	14
2.667	64
2.624	14
2.566	17
2.554	21
2.334	11
2.130	14
2.113	14
1.925	14
1.896	10
1.869	21
1.661	19
1.648	10
1.607	26
1.601	11
1.597	43
1.586	29
1.583	17
1.569	14

^a Interplanar spacing.

^b Relative intensity.

TABLE 4. X-ray diffraction powder data for the high temperature modification of $Gd_2O_3 \cdot TiO_2$ ^a (CuK α radiation)

hkl ^b	d ^c	1/d ²		I/I ₀ ^e
		Obs	Cal ^d	
002	6.02	0.0276	0.0277	10
100	3.189	.0983	.0983	38
101	3.083	.1052	.1056	32
	3.0435	.1080		10
004	3.007	.1105	.1112	26
102	2.817	.1260	.1264	100
104	2.185	.2094	.2098	22
105	1.918	.2720	.2724	8
110	1.839	.2958	.2958	29
112	1.757	.3239	.3236	8
106	1.694	.3484	.3488	12
200	1.645	.3944	.3944	58
201	1.578	.4017	.4014	10
114	1.568	.4070	.4070	59
202	1.538	.4227	.4222	60
212	1.1801	.7183	.7181	8
300	1.0612	.8881	.8875	8

^a Specimen not single phase. The line which occurs at $d=3.0435$ Å probably represents a metastable phase formed only in the quenched liquid.

^b Hexagonal Miller indices.

^c Interplanar Spacing.

^d Based on a hexagonal cell, $a=3.683$ Å, $c=11.995$ Å.

^e Relative intensity.

$\cdot 2TiO_2$ ($a=10.055$ Å) and $Lu_2O_3 \cdot 2TiO_2$ ($a=10.023$ Å). Subsequent work by Brixner [4] confirmed these earlier data.

The eutectic between $Gd_2O_3 \cdot 2TiO_2$ and TiO_2 is shown (fig. 1) as occurring at approximately 86 mole percent TiO_2 . Some difficulty was encountered in establishing the liquidus curves near the eutectic composition because it was virtually impossible to distinguish a partially melted from a completely melted specimen. For this reason, the eutectic composition shown in fig. 1 was approximated. Since the melting point of TiO_2 was not redetermined the liquidus was dashed from the eutectic composition to approximately 100 percent TiO_2 .

5. Summary

The phase equilibrium diagram for a major portion of the Gd_2O_3 - TiO_2 system has been determined from a study of solid state reactions and melting point relations.

A platinum alloy quenching furnace was used to establish all of the subsolidus and some of the liquidus relationships below 1800°C. An inductively heated iridium crucible was used for the determination of solidus and liquidus relationships above 1800°C. Phases were identified by x-ray powder diffraction and polarizing microscopic techniques.

Three intermediate phases were formed in the system. A solid solution phase is indicated on the phase diagram as existing from 33 to 40 mole percent TiO_2 , at 1750°C. This phase melts incongruently over a range of temperatures and compositions varying from 1840°C, the peritectic temperature, at 35 mole

percent TiO_2 to 1775°C, at 40 mole percent TiO_2 the incongruent melting temperature of $Gd_2O_3 \cdot TiO_2$. The minimum temperature of stability for the phase is 1600°C at 38 mole percent TiO_2 . The x-ray diffraction pattern of the solid solution phase was indexed on the basis of a face-centered cubic cell with unit cell dimension varying from about 5.28 Å to 5.32 Å at 1750°C. The second phase, a 1:1 compound, melts incongruently at 1775°C and has a reversible phase transition at 1712°C. The high temperature modification was indexed on the basis of a hexagonal cell related to the hexagonal rare earth oxides with $a=3.683$ Å, $c=11.995$ Å. The third phase, $Gd_2O_3 \cdot 2TiO_2$, melts congruently at 1820°C. This phase apparently accepted up to about 3 mole percent TiO_2 in solid solution at 1460°C. The unit cell dimensions of this pyrochlore structure type were found to vary from approximately 10.181 Å to 10.169 Å. From x-ray powder diffraction data the equimolar compositions of either Sm_2O_3 or Eu_2O_3 with TiO_2 were found to form phases which were very similar to both the low and high temperature modifications of $Gd_2O_3 \cdot TiO_2$. The composition $Dy_2O_3 \cdot TiO_2$ apparently formed several phases one of which was apparently similar to the high temperature form of $Gd_2O_3 \cdot TiO_2$.

6. References

- [1] S. J. Schneider, R. S. Roth, and J. L. Waring, J. Res. NBS **65A** (Phys. and Chem.) No. 4, 345-374 (1961).
- [2] J. B. MacChesney and H. A. Sauer, J. Am. Ceram. Soc. **45**, No. 9, 416-422 (1962).
- [3] R. S. Roth, J. Res. NBS **56**, No. 1, 17-25 (1956) RP2643.
- [4] L. H. Brixner, Inorg. Chem. **3**, No. 7, 1065-67 (1964).
- [5] F. Queyroux, Bull. Soc. Franc. Mineral. Crist. **86**, No. 3, 295-296 (1963).
- [6] R. S. Roth and S. J. Schneider, J. Res. NBS **64A** (Phys. and Chem.) No. 4, 309-316 (1960).
- [7] R. Roy, I. Warshaw, and Y. Ukai, Third Quarterly Progress Report on Crystal Chemistry Studies. (Oct. 1, 1960-Dec. 30, 1960), File No. 40608-P-M-60-93-93, The Pennsylvania State University, 1-104 (1961).
- [8] M. Perez y Jorba, Thèses Contribution à l'étude des systèmes zircone-oxyde de terres rares. Faculté Des Sciences De L'Université De Paris 1-33 (1962).
- [9] Swanson and Tatge, NBS Circ. 539, Vol. **I**, 44 (1953).
- [10] H. F. Stimson, J. Res. NBS **65A** (Phys. and Chem.) No. 2, 139-145 (1961).
- [11] S. J. Schneider and J. L. Waring, J. Res. NBS **67A** (Phys. and Chem.) No. 1, 19-25 (1963).
- [12] F. A. Mauer, Bridge-type Furnance Controller using Brown Servoamplifier, Informal Communiation; see also R. H. Bogue, Chemistry of Portland Cement, 2d ed. p. 311 (Reinhold Publishing Corp., New York, 1955).
- [13] L. G. Wisnyi and S. Pijanowski, Metal Report of Tech. Dept., Mar., Apr., and May. U.S. AEC Publ. Kapl-1564, 19-20 (1956).
- [14] C. E. Curtis and J. R. Johnson, J. Am. Ceram. Soc. **40**, 15-19 (1957).
- [15] S. J. Schneider, NBS Monograph 68 (1963).
- [16] J. L. Waring and S. J. Schneider, Bull. Amer. Ceram. Soc. **43**, No. 4, 263 (1964).

(Paper 69A3-344)